Supplementary Information

Cross-linker Free Sodium Alginate and Gelatin Hydrogel: Multiscale Biomaterial Design Framework

Tithi Basu[a#], Utkarsh Bhutani[ab#] and Saptarshi Majumdar[a]*

[a]Department of Chemical Engineering, Indian Institute of Technology Hyderabad, Sangareddy, Telangana 502285, India

[b]Institute for Stem Cell Science and Regenerative Medicine, NCBS-TIFR, GKVK-Campus, Bellary Road, Bangalore, 560 065, India

[#]T.B. & U.B. contributed equally to this paper

[*]E-mail: saptarshi@che.iith.ac.in

S1 MATERIALS AND METHODS

S1.1 Materials

Sodium alginate (SA; high viscosity, 1000–1500 cps, 1% in water), gelatin (G) (Type A, 175 bloom; isoelectric pH 7-9), Polyethylene glycol (PEG 2000), glycerol (99%), and naproxen sodium were procured from Alfa Aesar and used as received. Sodium chloride (NaCl), potassium chloride (KCl), sodium hydrogen phosphate (Na_2HPO_4, ACS 99%), and potassium dihydrogen phosphate (KH_2PO_4, ACS 99%) were used for the preparation of phosphate buffer saline (PBS, pH 7.4) and were also obtained from Alfa Aesar (Thermo Fisher company). Deionized water (DI) (Model: Milli Q, Millipore Elix water system, resistivity 18 MΩ cm) was used throughout the experiments.

S1.2 Preparation of Sodium Alginate and Gelatin Hydrogels

Gelatin (1.6 g) was dissolved in water (20 mL) at 60^{o}C and was allowed to form a homogenous solution. PEG 2000, NaCl, and glycerol were added sequentially. The composition (PEG, NaCl, and glycerol) were varied as per the experimental requirements, while the ratio of SA/G (Sodium Alginate/Gelatin) was fixed at 60/40 (w/w). Naproxen sodium (30 mg) was added (after glycerol) during the preparation of drug-loaded hydrogels. Once these components were extensively stirred, SA (2.4 g) was added and dried at 37^{o}C that led to the formation of hydrogels. These hydrogels were then dried and used for further studies. Similarly, 50/50, 70/30 and 75/25 SA/G hydrogels were also prepared.

S1.3 Small Angle X-ray Scattering (SAXS)

Gelatin (1.6 g) solutions were prepared in water (20 mL) at 40°C. Once a homogeneous solution was formed, PEG 2000 was added with a varying amount (0.5 g to 1.5 g). The SAXS analysis was performed, and the scattering time was set to 20 minutes (SAXSess, Anton Paar, Cu X-ray source). The intensity *I(q)* versus wave vector *q* data was obtained and analyzed.

$$q = \frac{4\pi n}{\lambda} sin(\theta/2) \quad \text{(S1)}$$

Where, θ = scattering angle, λ = radiation wavelength.

A similar procedure was followed for NaCl (50 mg to 400 mg) and glycerol (0.5 mL to 2 mL). To further explore their combined effect, PEG, NaCl, and glycerol were added sequentially, exactly following the hydrogel preparatory method (sequential addition) and SAXS was performed at each step.

These data were used to calculate the pair distribution function *p(r)* using indirect Fourier transform (IFT) (**equation S2**). The radius of gyration, R_g was calculated from the pair distribution function within the range of maximum particle dimension D_{max} (**equation S3**) [1]. All these analyses were performed using the GIFT (Generalized Indirect Fourier Transform) software from the PCG software package.

$$p(r) = 4\pi \int_0^{\infty} I(q)\, qr \sin(qr)\, dq \quad \text{(S2)}$$

$$R_g^2 = \frac{\int_0^{D_{max}} r^2\, p(r)\, dr}{2\int_0^{D_{max}} p(r)\, dr} \qquad where, D \leq \frac{\pi}{q_{min}} \quad \text{(S3)}$$

S1.4 Dynamic Light Scattering (DLS)

The gelatin solutions were prepared using the same protocol as for SAXS. 2 mL of solution was collected and the size of gelatin 'clusters' was analyzed using dynamic light scattering (Delsa Nano C, Beckman Coulter).

The scattering angle was fixed at 165° while the laser wavelength was 658 nm. CONTIN algorithm was used for data processing. The hydrodynamic radius, R_h was calculated via the Stokes-Einstein equation (**equation S4)** [2,3].

$$D = \frac{k_B T}{6\pi\eta R_h} \quad \text{(S4)}$$

Where, D = Translational Diffusion Coefficient, k_B = Boltzmann Constant, T = Temperature, η = Viscosity of the solution, R_h = Hydrodynamic Radius.

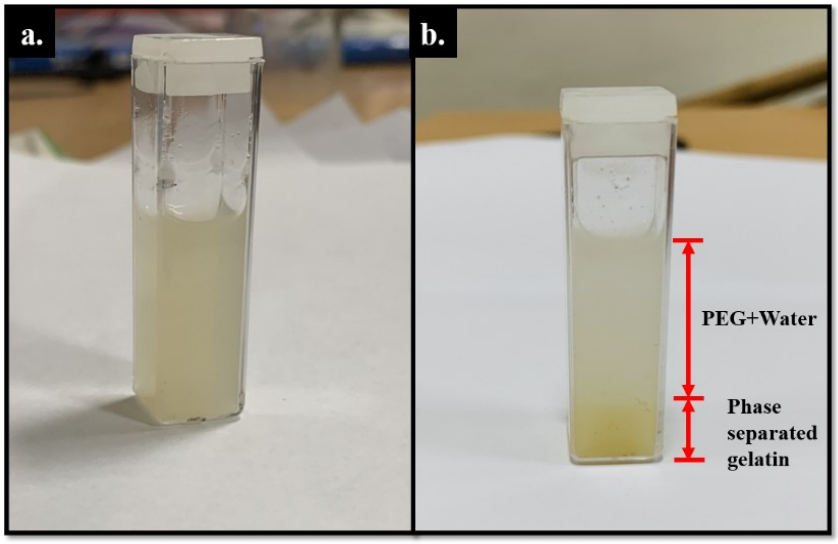

Figure S1. Gelatin + PEG solution. a) Turbid solution. b) Phase separated solution at 2 g PEG. This picture corroborates the effect of PEG 2000 on gelatin chains. Here, gelatin creates its own domain, and PEG is unable to enter this domain.

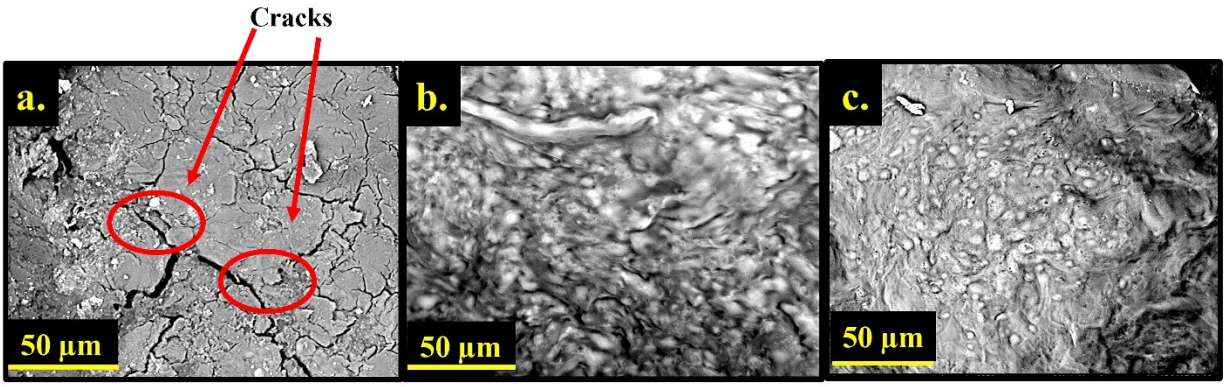

Figure S2. SEM (Scanning Electron Microscopy) images of 60/40 hydrogels. a) SA/G/ PEG (0.5 g). b) SA/G/ NaCl (100 mg). c) SA/G/ Glycerol (1.5 mL). Cracks were observed for the SA+ gelatin+ PEG case. The presence of PEG decreases the water diffusion inside the gelatin matrix that resulting in crack formation on the dried gel surface.

S1.5 Simulation methodology

All the MD (molecular dynamics) simulations were performed using the software GROMACS (GROningen Machine for Chemical Simulation, version 2019.5) [4]. The atoms in polymers were treated with OPLSAA forcefield with periodic boundary conditions in all three dimensions while SPC/E water model was chosen for the water molecules [5]. These parameters were chosen as they give much more realistic results when compared with experiment (for liquid water) [6]. The initial

configurations were prepared using Avogadro (version 1.2.0) software [7]. In this software, SMILES (Simplified Molecular Input Line Entry System) text was used as an input to generate the molecular structure. The GROMACS topology was generated using TopolGen (version 1.1). This script provides an initial topology file that requires modifications. The modifications were done by building script files for each polymer molecule. For visualizing the molecular structure, VMD (Visual Molecular Dynamics, version 1.9.3) software was used [8]. The energy minimization was performed for each system using the steepest descent algorithm until a maximum force of lesser than 1000 KJ/mol/nm was reached. This was done to avoid any steric repulsions in the system. A 5 ns NVT simulation was conducted with the energy minimized structure, followed by a 10 ns MD production. The leapfrog algorithm was used to integrate the equation of motion and the time step used as 1fs. LINCS algorithm was employed to constrain all the bonds [9]. The system temperature was maintained at 310 K using the Nosé-Hover thermostat [10]. The long-range electrostatic interactions were computed using particle mesh Ewald (PME) method [11]. The cut-off distance for van der Waals and the short-range electrostatic interactions were taken as 1 nm. The evolution of the radial distribution function (RDF) of the system with time (for every nanosecond) was used as a criterion to check if the system has equilibrated. The simulation trajectory of the MD production run for the last 1000 time frames separated by 5 ps was used to calculate the average over all the statistics. Five gelatin chains of molecular weight 8000 g/mol were used. The box length was chosen equivalent to the experimental 8% w/v concentration. To mimic the experimental set-up, at first dry gelatin chains were simulated and then the final conformation was simulated in presence of explicit water molecules. To maintain the sequential addition protocol of the experiments, PEG, NaCl, and glycerol were added one by one to the final simulated state of each case. The isoelectric point of gelatin type A ranges between 7 to 9 [12,13]. In the simulation the isoelectric point is taken as pH 7. The number of positive and negative charges are equal and the net charge on the polymer is zero at pH 7. The amino acid sequence of gelatin monomer is as follows:
—Proline-Glycine-Hydroxyproline-Glutamic Acid-Glycine-Arginine-Proline-Glycine-Alanine—
The snapshot of a gelatin monomer is shown in **figure S3**. The polymerization degree for PEG was taken as 45. The molecular weight of a single PEG chain is 2000 g/mol. The structural image of PEG monomer and glycerol can be seen in **figure S4**.

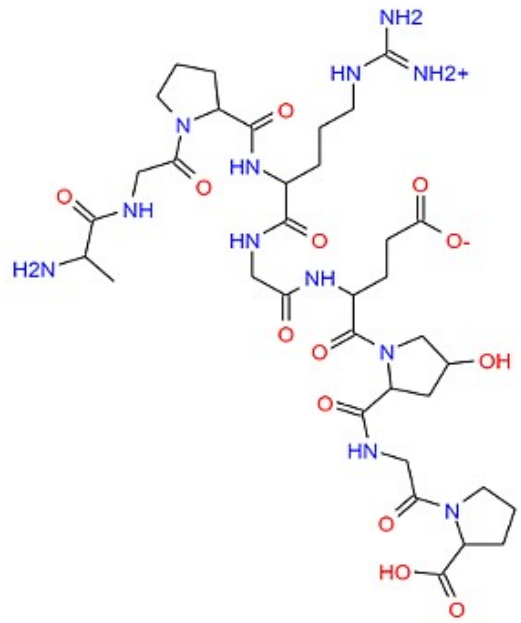

Figure S3: Snapshot of a single gelatin monomer structure used for MD simulation.

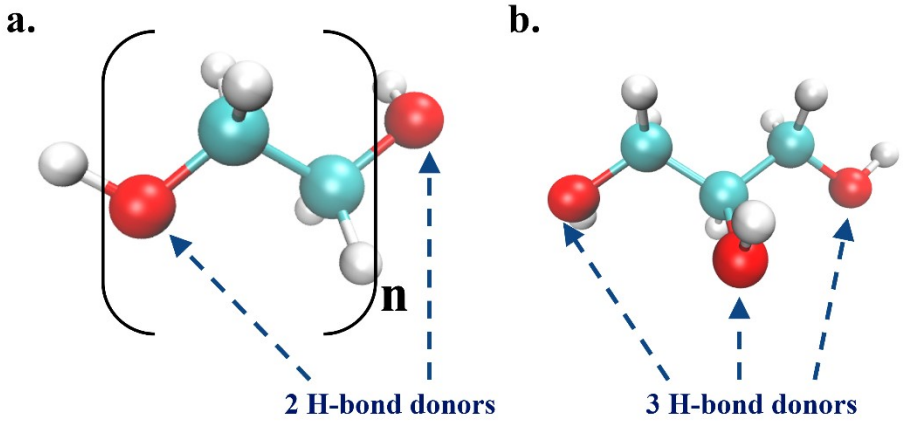

Figure S4: Snapshot of structure used for MD simulation: The backbone C-atoms are represented with cyan color beads; white color beads represent H-atoms, and red color beads represent O-atom. **a.** PEG monomer: n representing the number of repeating units. **b.** Glycerol molecule.

S1.6 Fourier Transform Infrared Spectroscopy/Attenuated Total Reflectance (FTIR/ATR)

The structural modifications incurred by gelatin during the preparation of hydrogels were identified using FTIR-ATR spectroscopy. 8% (w/v) gelatin samples were prepared and dried at 25°C. The individual effects and the combined effects (sequential addition) of PEG, NaCl, and glycerol were identified. The FTIR-ATR analysis was performed using Bruker Tensor 37, MIRacle Single Reflection Horizontal ATR accessory. The spectral range was collected between 600-4000 cm^{-1} with a spectral resolution of 4 cm^{-1}. 256 scans were performed to ensure the reproducibility of the data. The full FTIR/ATR spectra were normalized with respect to the asymmetric stretch of the CH_2 group at 2925 cm^{-1} [14]. FTIR spectroscopy is a powerful technique

to characterize protein secondary structures. The changes in gelatin (protein) secondary structure was monitored carefully via deconvolution protocol. The second derivative of amide I (1600-1700 cm^{-1}) spectra was calculated using the Savitsky-Golay algorithm in OriginPro9 [15].

S1.7 Swelling Behavior

The swelling degree (SD) of dried hydrogels was measured gravimetrically by placing the hydrogels in PBS (pH 7.4) at 37°C. The SD was calculated using the equation below

$$SD(\%) = \frac{(W_s - W_d)}{W_d} X100 \quad \text{(S5)}$$

Where W_s is the weight of swollen hydrogel and W_d corresponds to the weight of the dry hydrogel. The weights of the swelled hydrogels were measured at specific time intervals (0, 30, 60, 120, 240, 360, 480, 600, 720, 1440, 2880 min). The hydrogels were removed from the PBS and carefully wiped using tissue paper to reduce the excess water on the surface and weighed using a microbalance (Sartorius CPA26P). The experiments were carried out in triplicates and the standard deviations were calculated.

S1.8 In Vitro Controlled Release Studies

The drug (naproxen) loaded hydrogels were subjected to in-vitro drug release studies in PBS (pH 7.4). This solution mimics the environment of our intestine, where the absorption of the drug takes place. The hydrogels were immersed in PBS solution (100 mL) at 37°C and stirred continuously at 100 rpm. 3mL aliquots were collected at specific time intervals, the solution was replenished with an equivalent amount of fresh PBS (3mL) to maintain the sink conditions. The aliquots were analyzed using UV–VIS spectroscopy (Lambda 35, Perkin Elmer). The absorbance values for naproxen sodium were recorded at 272 nm (λ_{max}). Apart from calculating the cumulative drug release, this study was carefully aimed at monitoring the zero-order release kinetics. To monitor the zero-order release, release factor (RF) was defined, also published in our previous research [16].

$$RF = Release\ Fraction\ (RFN) X\ Time\ Fraction\ (TFN)\ X\ \ R^2 \quad \text{(S6)}$$

The cut-off for calculating the release factor was the period (time) up to which the zero-order release kinetics was observed i.e. R^2 ~0.99. R^2 value assures the smoothness of the release profile, which is also an important factor to be controlled.

$$RFN = \frac{Amount\ of\ Drug\ Release\ (mg)\ until\ zero\ order\ Kinetics}{Total\ Amount\ of\ Drug\ Loaded\ (mg)\ in\ the\ hydrogels} \quad \text{(S7)}$$

$$TFN = \frac{Time\ (h) until\ which\ zero\ order\ Kinetics\ was\ observed}{Total\ Time\ for\ Drug\ release\ (h)} \quad \text{(S8)}$$

S1.9 Statistical Analysis

All the data are represented as mean ± standard deviation with three replicates. Statistical analysis was carried out with a two-tailed Student's *t*-test to analyze the difference between two treatment means. The two treatments are defined as in vitro controlled release experiments performed with pure SA/G hydrogel (without PEG, NaCl, glycerol) and with PEG, NaCl, and glycerol. The null hypothesis was stated as "There are no significant differences in between two treatment means". The results were statistically significant with $p < 0.05$.

S1.10 Designing the 2D (two-dimensional) Plot

Swelling degree is an innate attribute of hydrogels that further governs the controlled diffusion of drug molecules. At pH 7.4, the sodium alginate chain is in an expanded state, gelatin is near its isoelectric point (pH 7-9), so it is in a collapsed state. As mentioned before, sodium alginate works as a shell protecting the gelatin core inside it. The gel is physically cross-linked and the gelatin will not degrade immediately unless the total gel degrades, which can be observed from the swelling degree data. The 2D plot was designed in such a way that NSD (Normalized Swelling Degree) and NRF (Normalized Release Fraction) [16] can be brought under the same roof (**Figure S5**a). The x-axis depicts NSD. It is the ESD (Equilibrium Swelling Degree), where the swelling curve saturates, i.e. the gel is swelled to its maximum capacity. The y-axis depicts the NRF. NRF denotes the amount of drug released for a time up to which zero-order kinetics is observed with respect to the total time taken to release the total amount of loaded drug. It is a mathematically defined factor that ensures and attempts to quantify a correct zero-order release profile for naproxen sodium.

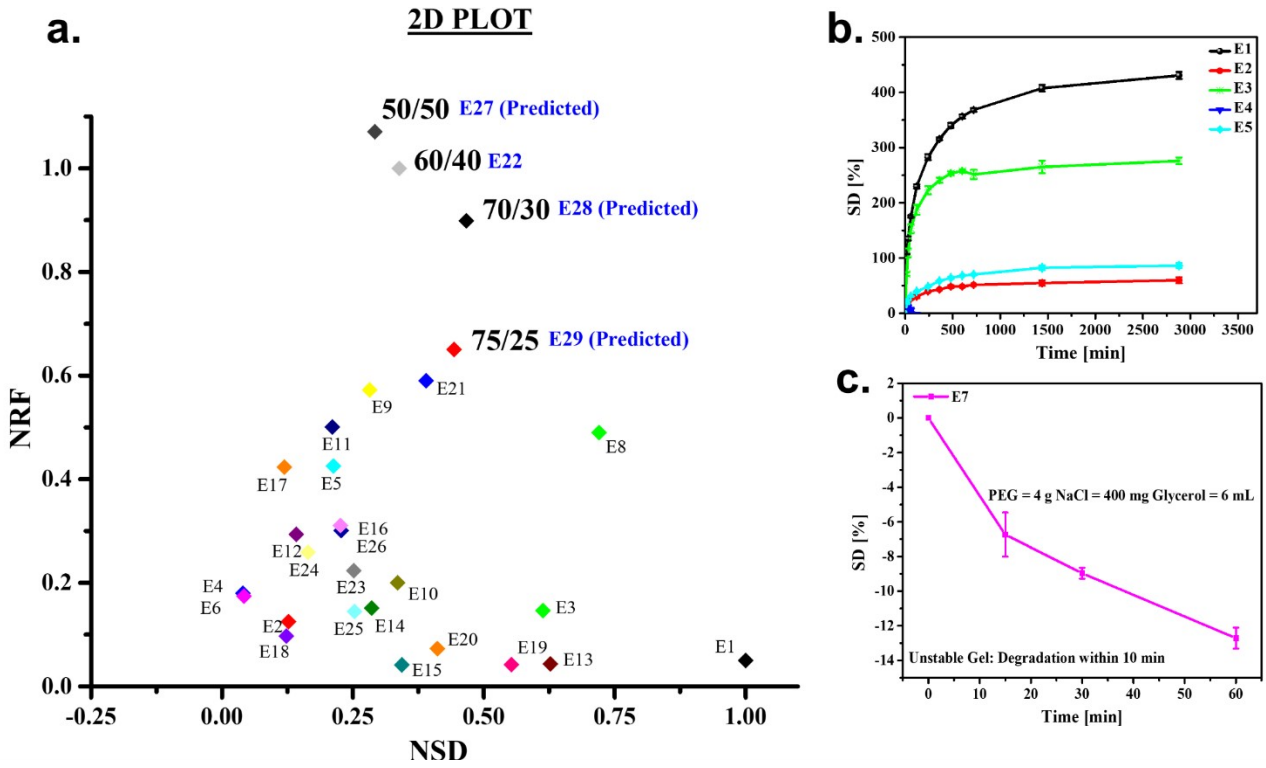

Figure S5. a) 2D plot (Total experimental sets). This plot features the central theme of this research depicting the stability (NSD) and release (NRF) of the hydrogels, which helps in identifying the finest samples. b) Swelling degree for a few selected samples. c) Swelling Degree: E7/1.

The investigation started with pure SA and gelatin hydrogel (absence of PEG, NaCl, and glycerol). This case recorded the highest ESD = 430.72 (E1, **Figure S5**b). The entire swelling data was normalized w.r.t it, giving us NSD. However, the drug release was below par. SA and gelatin alone form inhomogeneous hydrogels, leading to a non-uniform distribution of naproxen in the hydrogel core. This resulted in major naproxen localization near or close to the hydrogel surface culminating in a burst release (24 of 30 mg in 6 h, NRF = 0.05). This inhomogeneous distribution of the current hydrogels demanded more pliability, which was imparted by plasticizers (PEG & glycerol) and NaCl thereafter. The initial study revealed that the hydrogel with PEG (4 g), NaCl (400 mg) and glycerol (6 mL) degraded drastically within 30 minutes (E7/1, **Figure S5**c). The reason behind this was the excessive plasticization of the hydrogel which led to the breakage of the labile bonds. This was highly undesirable, however, this experiment enabled us to identify the specific search domain with respect to NSD. The pure SA/G hydrogel (without any other component) (highest SD) and the hydrogel with both the plasticizers and NaCl (poorest SD) were marked as the two extremes in the 2D plot.

Table S1. Experimental Sets for SA/G (w/w) Hydrogels ($p < 0.05$)

SA	*Gelatin*	*Experiment*	*PEG (g)*	*NaCl (mg)*	*Glycerol (ml)*	*NSD*	*NRF*
60	40	E1	0	0	0	1	0.0501
60	40	E2	4	0	0	0.127	0.12515
60	40	E3	0	400	0	0.61296	0.14646
60	40	E4	4	400	0	0.03993	0.17995
60	40	E5	0	0	6	0.21291	0.42543
60	40	E6	4	0	6	0.04207	0.17426
60	40	E7	4	400	6	0	0
60	40	E8	0	200	0	0.72	0.49
60	40	E9	0	0	3	0.28196	0.57258
60	40	E10	0	200	3	0.33515	0.20029
60	40	E11	0	400	3	0.21047	0.5006
60	40	E12	0	200	6	0.14163	0.29348
60	40	E13	0	100	1.5	0.62689	0.04351
60	40	E14	0	200	4.5	0.28558	0.15141
60	40	E15	0	500	3	0.34363	0.04153
60	40	E16	0	400	4.5	0.22754	0.30089
60	40	E17	0	600	6	0.11922	0.42326
60	40	E18	0	800	6	0.12306	0.0973
60	40	E19	0	0	1.5	0.5528	0.04182
60	40	E20	1	200	0	0.41112	0.0728
60	40	E21	1	100	1.5	0.39	0.59
60	**40**	**E22**	**0.5**	**100**	**1.5**	**0.33852**	**1 (24 h)**
60	40	E23	1	50	1.5	0.25168	0.22371
60	40	E24	1	150	1.5	0.16424	0.25931
60	40	E25	1	100	1	0.25308	0.14479
60	40	E26	1	100	2	0.22631	0.31056
50	**50**	**E27**	**0.895**	**125**	**1.105**	**0.29208**	**1.07063 (48 h)**
70	**30**	**E28**	**0.11**	**75**	**1.81**	**0.46668**	**0.89877**
75	**25**	**E29**	**0**	**62.5**	**2.076**	**0.44346**	**0.65029**

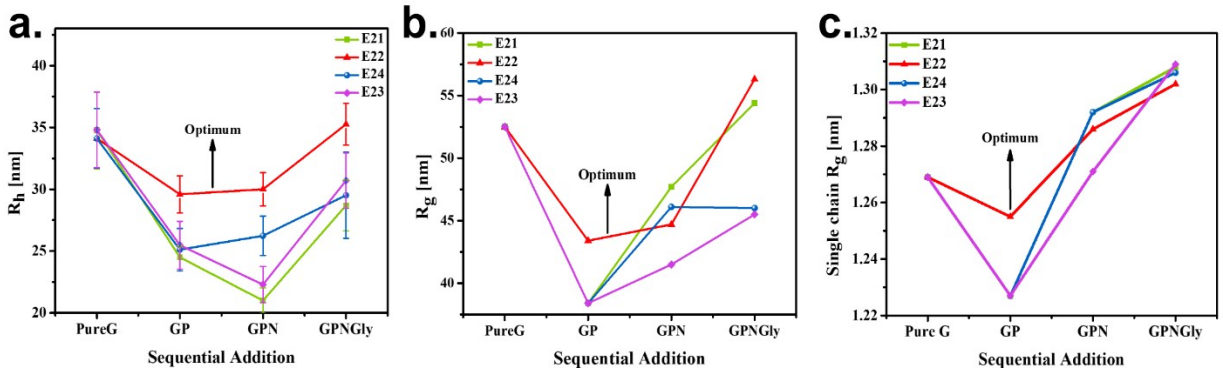

Figure S6. Variation in gelatin chain size upon sequential addition for optimum and non-optimum samples. a) R_h. b) R_g. c) Single-chain R_g from MD simulation G (gelatin) P (PEG) N (NaCl) Gly (glycerol). In every case, there is a collapse and re-expansion upon PEG addition.

S1.11 Dimensionless Parameter Calculation

The optimum sample data [PEG (0.5 g), NaCl (100 mg), and glycerol (1.5 mL), (glycerol density: 1.26 gm/cc)] was used as the basis for calculating the parameters *P1* and *P2*.

$$P1 = \frac{NaCl}{Gelatin} = \frac{100\ mg}{1600\ mg} = 0.0625 \quad \text{(S9)}$$

$$P2 = \frac{(PEG + 1)}{(Glycerol + 1)} X \frac{SA}{Gelatin} = \frac{(0.5 + 1)}{(1.89 + 1)} X \frac{2.4}{1.6} = 0.78 \quad \text{(S10)}$$

Based on the overall amount of the plasticizers [PEG (0.5 g) and glycerol (1.89 g)] obtained for the best case, an assumption was made in such a way so that the total amount of plasticizers remains constant from case to case and experiments are done accordingly for other SA/G ratios:

$$PEG + Glycerol = 2.4 \quad \text{(S11)}$$

A sample calculation for 70/30 (2.8 g SA & 1.2 g Gelatin) hydrogels is given below:

$$P1 = 0.0625 = \frac{NaCl}{1200\ mg}\ \ i.e.\ NaCl = 75\ mg \quad \text{(S12)}$$

$$P2 = \frac{(PEG + 1)}{(Glycerol + 1)} X \frac{SA}{Gelatin} = \frac{(PEG + 1)}{(Glycrol + 1)} X \frac{2.8}{1.2} = 0.78 \quad \text{(S13)}$$

Solving for *P2* we get:

$$2.34\ (Glycerol) - 7\ (PEG) = 4.66 \quad \text{(S14)}$$

Thus solving the above equation along with the assumed equation (total amount of both plasticizers remains the same for all the cases), the values of PEG and Glycerol were obtained. Thus the

amounts of PEG, NaCl and glycerol for 70/30 hydrogels obtained via dimensionless parameters were:

$$PEG \approx 0.11\ g, NaCl \approx 75\ mg, Glycerol \approx 1.81\ mL$$

Similarly, the amounts PEG, NaCl, and glycerol obtained for 50/50 and 75/25 hydrogels is given below:

50/50

$$PEG \approx 0.895\ g, NaCl \approx 125\ mg, Glycerol, \approx 1.105\ mL$$

75/25

$$PEG \approx 0\ g, NaCl \approx 62.5\ mg, Glycerol \approx 2.076\ mL$$

The 75/25 SA/G hydrogel NRF value was not at par with that of 60/40 and 50/50 SA/G hydrogel due to the higher viscosity of SA. That's why the 80/20 (80 wt% SA) hydrogels were not tested in this study. The other question that arises here is the fate of hydrogels below 50/50. The cases below 50/50 hydrogels have a higher proportion of gelatin (40/60, 30/70, 20/80). These are often associated with early dissolution due to higher gelatin content. Hence the parameters predict well for hydrogels having a proportional amount of SA and gelatin. These linear equations are valid only when no new &/or significant physics is included or acting as dominating factors e.g. higher viscosity and faster degradation. The parameters are unable to incorporate the viscosity effect for very high SA i.e. 80/20 hydrogels, where viscosity can be a detrimental factor or cases below 50/50, where the dissolution is higher due to increased gelatin concentration.

S1.12. Rheological Properties

The rheological measurements were performed using Anton Paar Rheometer MCR 92. The selected optimum (E22, E27, E28) and non-optimum samples (E23, E24, E21, E1) were chosen along with the pure SA/G hydrogel and were allowed to swell for 24 h and evaluated for their rheological properties. The motive behind this analysis was to check the strength of the hydrogel and correlate them with the existing swelling degree data. An amplitude sweep analysis was performed with a varying shear strain ranging from 0.01% to 100% at 37 °C at a frequency of 1 Hz. A cone plate geometry of 25 mm diameter was used with a cone angle of 2° and a measurement gap of 0.105 mm was used for the testing. The storage modulus (*G'*) and loss modulus (*G''*) were measured (n = 3) to characterize the viscoelastic behavior of the crosslinker free hydrogels briefly. At the linear viscoelastic region, the storage modulus is higher than the loss modulus for each sample indicating the elastic nature of the gel (**Figure S7**). Here, only one such figure has been shown for the optimum sample (E22); all other samples follow similar phenomena. The storage modulus values obtained from the linear viscoelastic region were normalized similarly to the swelling degree data wrt the highest *G'* value. These data were then plotted against the NRF values of the selected optimum, non-optimum and pure SA/G hydrogels (**Figure S8**a). A similar resemblance of this plot was obtained with the earlier 2D plot of NSD/NRF (**Figure S8**b).

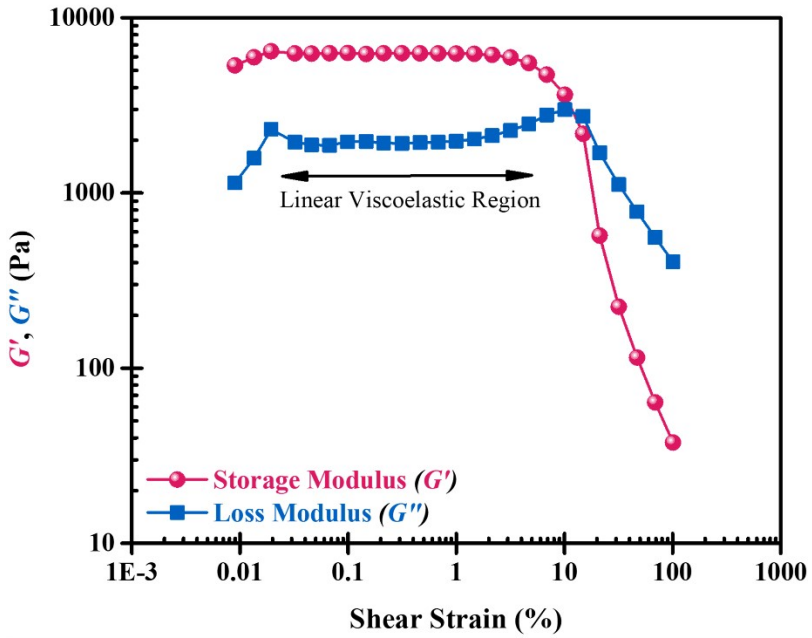

Figure S7. Storage modulus and loss modulus versus shear strain for the 60/40 optimum sample E22. The plot shows the linear viscoelastic region. Similar analyses were done for other samples.

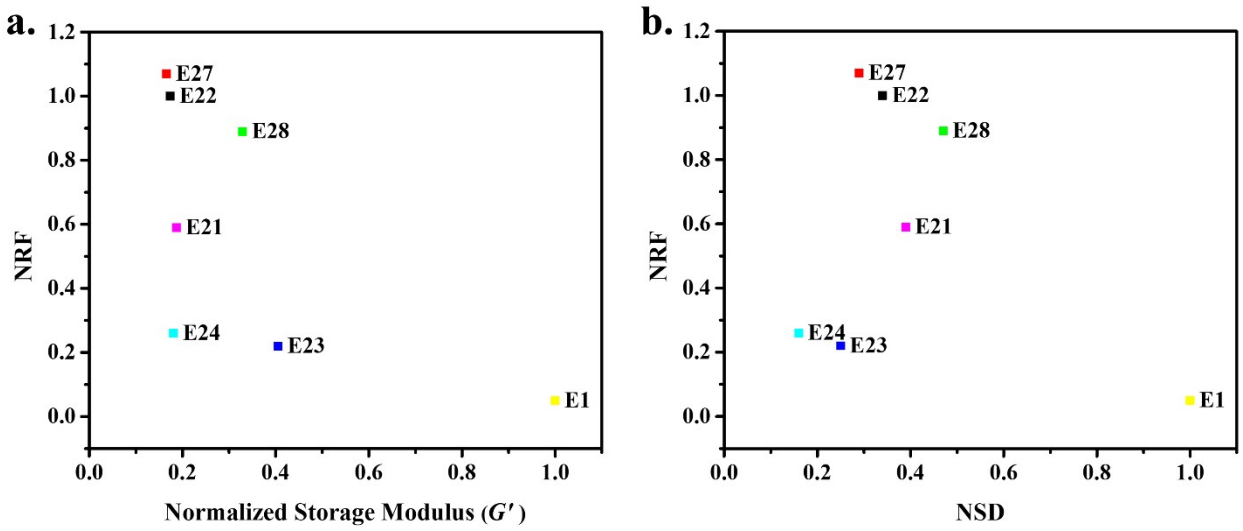

Figure S8. a) Normalized storage modulus (*G'*) versus NRF. b) 2D plot of NSD versus NRF for selected samples

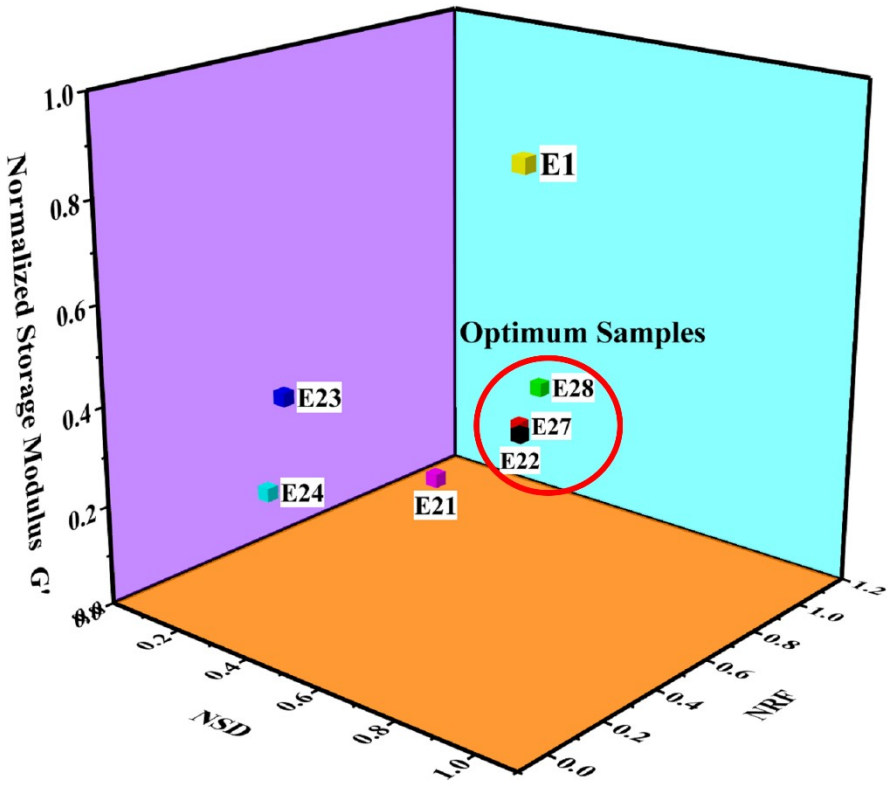

Figure S9. 3D plot of NSD-NRF-Normalized *G'*. Encircled mark shows that the optimum samples lie at the center of the plot.

S1.13 Characterization of other optimum samples

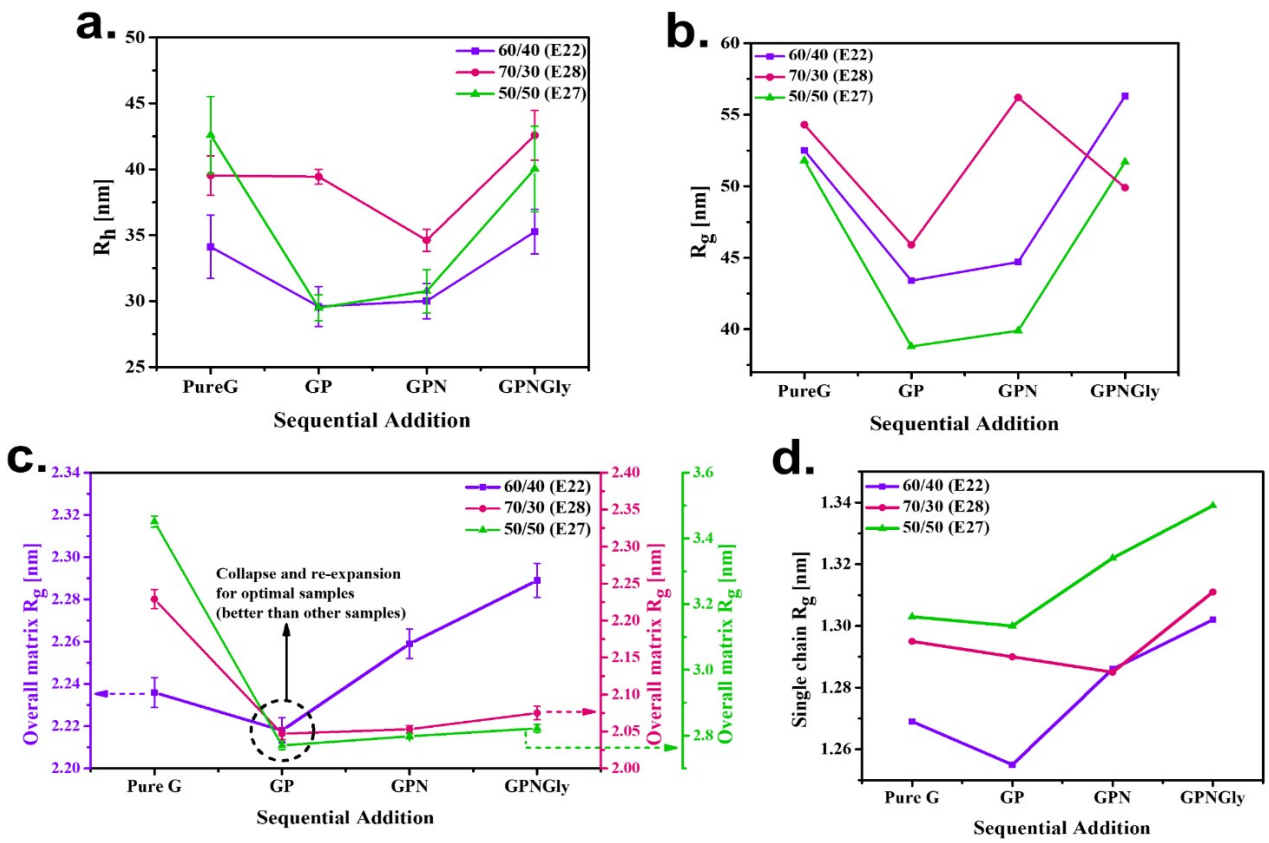

Figure S10. Gelatin size for the optimum samples with different SA/G ratios. a) R_h. b) R_g. c) Overall matrix R_g and d) Single-chain R_g from molecular simulation after 10 ns production run for the optimum cases.

Table S2. Simulation details for each experimental set-up

Experiment No.	*Number of gelatin chains*	*Number of PEG chains*	*Number of NaCl molecules*	*Number of glycerol molecules*	*Box length (nm)*
E21	5	12	43	513	9.4 * 9.4 * 9.4
E24	5	12	64	513	9.4 * 9.4 * 9.4
E23	5	12	21	513	9.4 * 9.4 * 9.4
E22	5	6	43	513	9.4 * 9.4 * 9.4
E27	6	11	53	378	9.4 * 9.4 * 9.4
E28	4	1	32	619	9.4 * 9.4 * 9.4

Table S3. NRF and R_h values for the selected experiment numbers

Experiment No.	*PEG 2000 (gm)*	*NaCl (mg)*	*Glycerol (mL)*	*R_h (nm)*	*NRF*
E22 (optimum)	**0.5**	**100**	**1.5**	**35.2 ± 1.7**	**1.00**
E21	1	100	1.5	28.7 ± 2.1	0.59
E23	1	50	1.5	30.7 ± 2.2	0.22
E24	1	150	1.5	29.5 ± 3.4	0.26
E13	0	100	1.5	37.9 ± 1.8	0.04
E8	0	200	0	67.1 ± 6.7	0.49
E5	0	0	6	56.2 ± 2.8	0.42
E11	0	400	3	53.1 ± 3.6	0.15

S1.14 Determination of gelatin shape through R_g/R_h ratio

To further understand the changes in size and shape of gelatin (protein), the ratio of the radius of gyration (R_g) to the hydrodynamic radius (R_h) was calculated. $R_g/R_h > 1.5$ predicts an elongated nature of protein while $R_g/R_h < 0.78$ indicates a globular structure [3] (**Figure S11**).

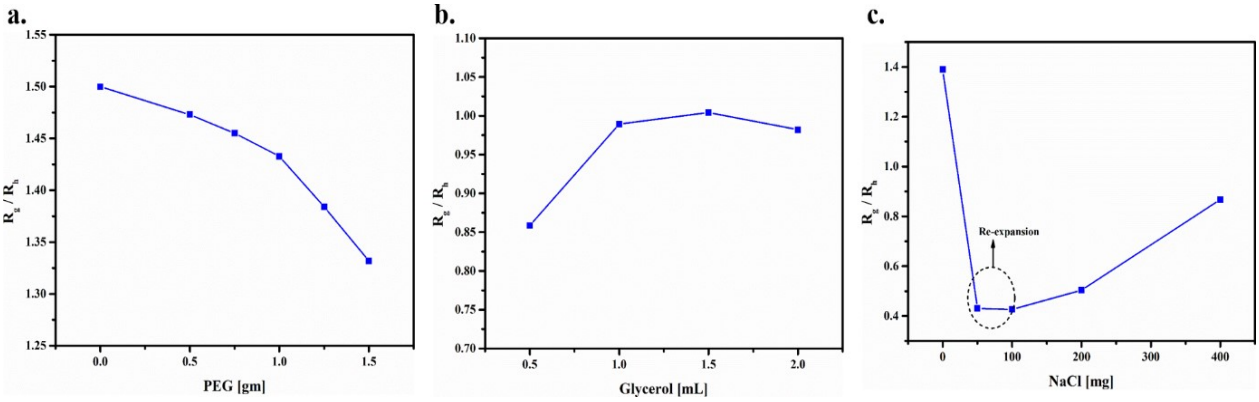

Figure S11. R_g/R_h ratio of gelatin in the presence of a) The R_g/R_h ratio was observed to decrease with an increasing amount of PEG indicating that the conformation starts moving from an elongated (1.5) towards a globular structure (1.35). A further decrease was not observed because the solution turns out turbid and phase separation occurs (**Figure S1**), b) Glycerol displayed an increase in the R_g/R_h values. As glycerol anchors to the gelatin chain with the help of hydrogen bonds, it extends the gelatin coil size, hence recording an increase in the R_g/R_h ratio, c) The re-

expansion phenomenon for gelatin-NaCl (observed in DLS and SAXS) is further confirmed by the R_g/R_h ratio. Initially, the ratio drops to 0.4 (50 mg NaCl) making the protein (gelatin) globular, while further addition of salt leads to an increased R_g/R_h (0.9) (400 mg NaCl) depicting an elongated state of gelatin, depicting the collapse-re-expansion behavior of gelatin [17].

S1.15 Quantification of Gelatin Mass Loss

The mass loss of gelatin from the physically crosslinked hydrogel was quantified using UV-VIS Spectrophotometer - LABINDIA UV-3092. The SA/G hydrogel samples were immersed in PBS solution at 37°C at 100 rpm. The UV absorbance values were checked at fixed time intervals. The percentage loss in gelatin mass was calculated from the UV absorbance value (Student's *t*-test $p < 0.05$).

Figure S12 represents the percentage mass loss of gelatin for: (a) the pure 60/40 SA/G hydrogel-E1 and the 60/40 optimum hydrogel-E22; (b) pure gelatin film. The gelatin percentage mass loss reached 22.5% (E1), 14.6% (E22) within 720 mins while 25.6% of the gelatin film was degraded in 90 mins. The gelatin film degraded after 2h, and 97% of total gelatin dissolved in the solution. Thus, this justifies that SA acts as a shell to the gelatin core. On the other hand, 2.23% of gelatin was lost within 30 mins from the hydrogel, and the swelling degree was 134-E1, 64-E22 (**Figure S13**). Hence, gelatin loss is low as the hydrogel is mostly swelling, and the drug is released via swelling in this case. At 1440 mins (24h) the mass loss of gelatin is 34.5% (E1), 25.8% (E22), and the swelling degree has almost saturated for both the hydrogel. This suggests that here the drug is released via degradation. The total mass loss of gelatin is 34.5% for the pure SA/G hydrogel and 25.8% for the optimum hydrogel after 24h. The mass loss percentage for the optimum sample is lesser than the pure SA/G hydrogel. Perhaps the controlled release was observed for the optimum sample as a lesser amount of gelatin was lost compared to the pure case.

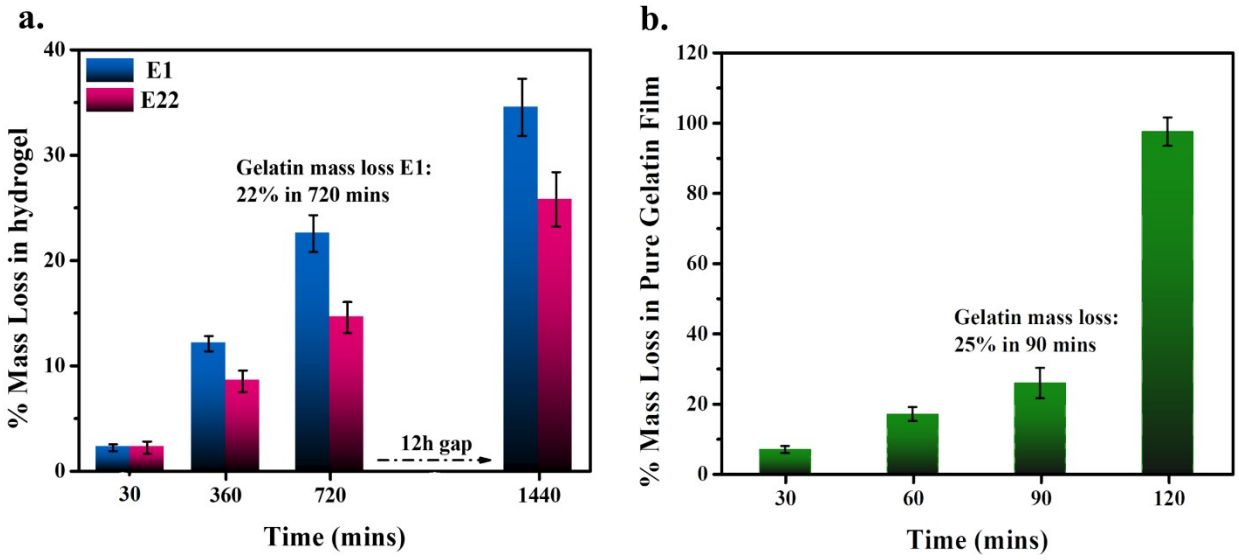

Figure S12. a) Cumulative percentage mass loss for pure 60/40 SA/G hydrogel (E1) and 60/40 optimum (E22) hydrogel. b) Cumulative percentage mass loss for pure gelatin film.

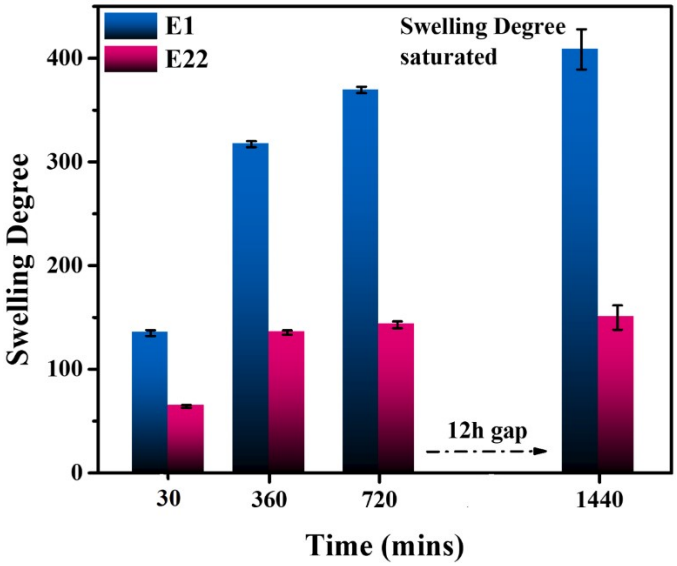

Figure S13. Swelling Degree for pure 60/40 SA/G hydrogel (E1) and 60/40 optimum (E22) hydrogel.

S1.16 Details of *β*-sheets and 3_{10}-helix

The hydrogen bond orientation between the amino hydrogen and carboxyl oxygen atoms determines the type of secondary structure. *α*-helices and *β*-sheets are the two most well-known secondary structures of the protein. 3_{10}-helices are observed at the ends of *α*-helices due to unfavorable backbone packing in the center of the helix and are also found to be a transitional conformation as *α*-helix tends to consistently fold and unfold. It is characterized by 3 residues per turn and 10 atoms are involved in ring formation by hydrogen bonds. The C=O group of i^{th} residue hydrogen bonds with the N-H group of $i+3^{th}$ residue, thus the name 3_{10}-helix. In contrast to that, *β*-sheets form a pleated sheet structure connected laterally by backbone hydrogen bonding [18].

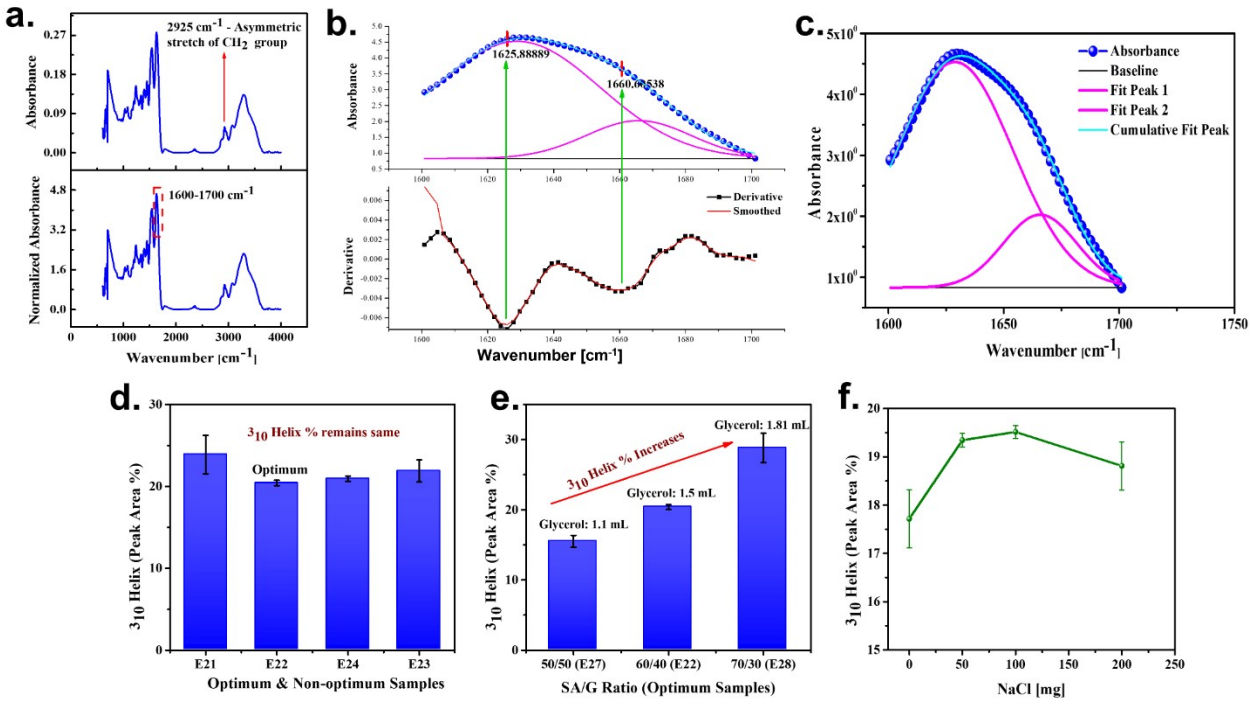

Figure S14. Deconvolution Protocol. a) FTIR/ATR absorbance spectra normalized w.r.t. 2925 cm^{-1} (asymmetric stretch of CH_2 group). b) the second derivative of the spectra (1600-1700 cm^{-1}). c) Two peaks at 1625 cm^{-1} and 1660 cm^{-1} were obtained for protein secondary structure analysis. 3_{10}-Helix peak area percentage: d) selected optimum and non-optimum samples, the final 3_{10} helix % remains the same as each of them includes 1.5 mL glycerol. b) optimum samples with different SA/G ratios, 50/50 (1.1 mL Gly), 60/40 (1.5 mL Gly), 70/30 (1.8 mL Gly). 3_{10} helix % increases with an increasing amount of glycerol. This implies that only glycerol can induce a large change in the 3_{10}-helix structure, proving its global plasticizing nature. g) Gelatin-NaCl.

References

1 A. G. Kikhney and D. I. Svergun, *FEBS Lett.*, 2015, **589**, 2570–2577.

2 J. Stetefeld, S. A. McKenna and T. R. Patel, *Biophys. Rev.*, 2016, **8**, 409–427.

3 S. Bhattacharjee, *J. Control. Release*, 2016, **235**, 337–351.

4 M. J. Abraham, T. Murtola, R. Schulz, S. Páll, J. C. Smith, B. Hess and E. Lindahl, *SoftwareX*, 2015, **1**–**2**, 19–25.

5 W. L. Jorgensen and J. Tirado-Rives, *J. Am. Chem. Soc.*, 1988, **110**, 1657–1666.

6 P. Mark and L. Nilsson, *J. Phys. Chem. A*, 2001, **105**, 9954–9960.

7 M. D. Hanwell, D. E. Curtis, D. C. Lonie, T. Vandermeersch, E. Zurek and G. R. Hutchison, *J. Cheminform.*, 2012, **4**, 17.

8 W. Humphrey, A. Dalke and K. Schulten, *J. Mol. Graph.*, 1996, **14**, 33–38.

9 B. Hess, H. Bekker, H. J. C. Berendsen and J. G. E. M. Fraaije, *J. Comput. Chem.*, 1997, **18**, 1463–1472.

10 W. G. Hoover, *Phys. Rev. A*, 1985, **31**, 1695–1697.

11 T. Darden, D. York and L. Pedersen, *J. Chem. Phys.*, 1993, **98**, 10089–10092.

12 C. Tapia, V. Corbalán, E. Costa, M. N. Gai and M. Yazdani-Pedram, *Biomacromolecules*, 2005, **6**, 2389–2395.

13 S. Gorgieva and V. Kokol, in *Biomaterials Applications for Nanomedicine*, InTech, 2011, pp. 1–36.

14 L. C. Sow and H. Yang, *Food Hydrocoll.*, 2015, **45**, 72–82.

15 H. Yang, S. Yang, J. Kong, A. Dong and S. Yu, *Nat. Protoc.*, 2015, **10**, 382–396.

16 U. Bhutani, A. Ronghe and S. Majumdar, *ACS Appl. Bio Mater.*, 2018, **1**, 1244–1253.

17 P. Swain, A. Ronghe, U. Bhutani and S. Majumdar, *J. Phys. Chem. B*, 2019, **123**, 1186–1194.

18 U. Langel, B. F. Cravatt, A. Graslund, N. G. H. von Heijne, M. Zorko, T. Land and S. Niessen, *Introduction to Peptides and Proteins*, CRC Press, 2009.